

EFFICIENT AND STABLE TIME INTEGRATION OF CAHN-HILLIARD EQUATIONS: EXPLICIT, IMPLICIT AND EXPLICIT ITERATIVE SCHEMES

© 2024 M.A. Botchev,^{1,*}, I.A. Fahurdinov,^{1,2,**}, E.B. Savenkov^{1,***}

¹ *Keldysh Institute of Applied Mathematics of Russian Academy of Sciences,
Miusskaya Sq. 4, Moscow, 125047, Russia*

² *National Research Nuclear University “Moscow Engineering Physics Institute” (MEPhI)
Kashirskoe Hw. 31, Moscow, 115409, Russia*

*e-mail: botchev@kiam.ru

** mv1451003@gmail.com

*** savenkov@keldysh.ru

Submitted --.2024

Revised version --.2024

Accepted for publication --.2024

To solve the Cahn-Hilliard equation numerically, a new time integration algorithm is proposed, which is based on a combination of the Eyre splitting and the local iteration modified (LIM) scheme. The latter is employed to tackle the implicit system arising each time integration step. The proposed method is gradient-stable and allows to use large time steps, whereas, regarding its computational structure, it is an explicit time integration scheme. Numerical tests are presented to demonstrate abilities of the new method and to compare it with other time integration methods for Cahn-Hilliard equation. Citations: 65. Figures: 5.

Key words: Cahn-Hilliard equation, gradient-stable schemes, Eyre splitting, local iteration modified scheme, LIM.

DOI:

1. INTRODUCTION

The Cahn-Hilliard equation was proposed in 1958 (see original paper [1]) to describe a phase separation in two-component alloys. Currently the equation is widely applied in various research fields and is one of the fundamental models in the so called gradient or weakly non-local thermo-mechanics of continuous media [2]. As a part of more complex models, the equation is employed in multiphase hydrodynamics, material science, solidification problems, phase transition theory and in many other fields [3, 4]. From a theoretical point of view, the Cahn-Hilliard equation forms the basis of phenomenological spinodal decomposition theory [5] and has a broad range of applications in theoretical physics, see [6–8] and references therein. Mathematics behind the Cahn-Hilliard equation is also widely discussed in the literature, see, e.g., [9].

Up to recently, the Cahn-Hilliard equation had been primarily seen as a theoretical tool in mathematical modeling of various processes. However, last decennia it has been actively employed also as a simulation tool, either independently or a part of more complex models. This has necessitated development of efficient numerical algorithms to solve the equation.

Difficulties arising in design of efficient numerical algorithms for the Cahn-Hilliard equation are mainly caused by the following two reasons. First, the Cahn-Hilliard equation is a nonlinear PDE

containing fourth order space derivatives. Due to nonlinearities, solutions of the Cahn-Hilliard equation evolve on a broad range of space and time scales. In particular, a typical solution is almost constant within the certain space regions of homogeneity which correspond to “pure” phases of the system. These homogeneity regions have a typical size d and are separated from each other by thin layers, of width $\epsilon \ll d$, the so-called “diffuse interfaces”, where the solution varies from its minimal to maximal values but remains smooth. At initial stages of spinodal decomposition, usually emerging due to a perturbation in the initial random distribution, the diffuse interface width ϵ is comparable to homogeneity region size d ($\epsilon \sim d$) and typical evolution times are of order ϵ^2 . However, in the course of further evolution, when the diffuse interface width becomes considerably smaller than the homogeneity region size, $\epsilon \ll d$, typical evolution times are of order $1/\epsilon$, see [10, 11].

As a consequence of these effects, explicit time integration schemes, being applied to the Cahn-Hilliard equation, are stable for time step sizes $\tau \sim h^4$, with h being the space grid size. Although such a restriction is physically motivated, in some cases it may turn out unacceptably strict for a computationally efficient solution process. At the same time, in fully implicit schemes, uniqueness of the solution on the next time level is not guaranteed for sufficiently large time step sizes [12, 13]. Therefore, design of numerical schemes which would be (a) uniquely solvable for arbitrary time steps, (b) stable, and (c) conservative, is not an easy task. Baseline algorithms meeting these requirements appeared relatively recently [14, 15]. They are based on a special splitting of system energy called convex splitting, see Section 3. We note that, in the context of numerical solution of the Cahn-Hilliard equation, “stability” usually means the so-called “gradient stability” (also known as “energy stability”), which guarantees that a discretized analogue of the system free energy does not grow with time, see Sections 2, 3 below. This stability condition can be considered as strong in the sense that the expression for the free energy includes first derivatives of solution. This is necessary to make sure that the numerical solution of the Cahn-Hilliard equation is thermodynamically consistent.

Currently, important research directions in efficient time integration of the Cahn-Hilliard equation include construction of adaptive numerical algorithms (needed due to the broad range of characteristic evolution times, as discussed above), development of energy-stable time integration schemes (producing thermodynamically consistent numerical solutions), and design of schemes which would be, on one hand, sufficiently asymptotically stable and, on the other hand, uniquely solvable and computationally efficient.

A complete review of current research on design and analysis of time integration schemes for the Cahn-Hilliard equation is far beyond the scope of this paper. An overview of main research directions in this field is given in a survey [16]. As examples of other relevant literature, we note [17–23] (adaptive and high-order methods), [24–26] (schemes, allowing “large” time step sizes), and [14, 15, 27–33] (energy-stable schemes).

To discretize the Cahn-Hilliard equation in space, various methods can be employed, such as classic finite difference methods, finite volume methods, spectral methods, standard and isogeometric finite element methods, see [34–47].

The aim of this paper is to study numerically a new class of time integration schemes for the Cahn-Hilliard equation. The new algorithms are based on two main ideas: (a) employment of implicit-explicit time integration schemes based on the convex splitting of the system energy [14, 15], ensuring the scheme is energy-stable, and (b) application of the local iteration modified (LIM) time integration scheme, which allows to combine the computational simplicity of explicit schemes with stability properties of implicit schemes. The Eyre splitting [14, 15] can currently be seen as a

basis for constructing time integration schemes for the Cahn-Hilliard equations, which should be both energy stable and uniquely solvable (meaning that the solution on the next time level in the time integration scheme exists and is unique).

Local iteration schemes form a family of explicit time integration methods, where stability is achieved by employing Chebyshev polynomials. Chebyshev polynomial iterations are used in time integration since at least the 1950s [48,49]. It should be emphasized that Chebyshev iteration in the local iteration schemes are used not to approximately solve linear systems arising in implicit time integration; if this would be the case then, as shown in 1952 by Gel'fand and Lokutsievskii (see [50] and [51, Ch.10, § 4.12]), no essential gain in computational work with respect to explicit schemes can be obtained. The key characteristic feature of the local iteration schemes is that Chebyshev iterations are constructed to ensure stability and accuracy of time integration, rather than to achieve a fast convergence to a solution of an implicit scheme. The local iteration schemes are proposed in [52–55] and further developed in [56–58], see also references in [58]. Specially tuned Chebyshev iterations allow the local iteration schemes to work with time step sizes essentially larger than in explicit Euler scheme, while keeping the computational simplicity of explicit schemes.

The first local iteration scheme proposed in [52–54] is not monotone (its numerical solution is not guaranteed to be nonnegative) and is not asymptotically stable for large times $t \rightarrow \infty$. Therefore here the local iteration modified (LIM) scheme, proposed in [55], is employed, which does have these properties. A detailed description and comparison of the local iteration schemes can be found in [58]. Up to date, the LIM scheme has been successfully applied to solve various rather challenging real-life problems, see, e.g., [59–61]. In [62], the LIM scheme is applied to solve the Cahn-Hilliard equation within a numerical implementation of a full mathematical model to describe metal crystallization processes. There, at each time step, the Cahn-Hilliard equation is linearized and the linearized problem is handled by the LIM method. No comparisons with other relevant time integration schemes are carried out in [62], and properties such as gradient stability are not investigated either.

In this paper, with a space one-dimensional Cahn-Hilliard equation taken as example, we propose new time integration schemes which are based the LIM scheme and implicit-explicit Eyre splittings. Results of numerical experiments, where the proposed methods are tested and compared to other time integration schemes, are presented.

In Section 2 a short description of the model is given. Currently used time integration schemes are briefly discussed in Section 3 and then, in the same section, new schemes are presented. Numerical experiments are described in Section 4. Finally, Section 5 summarizes results obtained in this paper.

Work of E.B. Savenkov is supported by by the Russian Science Foundation grant no. 2-11-00203.

2. MATHEMATICAL MODEL

We consider an one-dimensional (1D) Cahn-Hilliard equation

$$\frac{\partial c}{\partial t} = \frac{\partial}{\partial x} \left(M \frac{\partial \mu}{\partial x} \right), \quad \mu(c) = F'(c) - \epsilon^2 \frac{\partial^2 c}{\partial x^2}, \quad F(c) = c^2(1-c)^2, \quad (2.1)$$

where $c = c(x,t)$ is the unknown function, $M = M(c) > 0$ is a diffusional mobility coefficient (in all tests presented here we set $M \equiv 1$), $\mu = \mu(c, \partial c / \partial x)$ is a chemical potential, $\epsilon > 0$, $\epsilon = \text{const}$ is the diffuse interface width, t is the time, x the space variable.

Equation (2.1) is solved in a 1D domain $\Omega = (0,1)$ for $t \in (0,T]$. Boundary conditions

$$\frac{\partial c}{\partial x} = \frac{\partial \mu}{\partial x} = 0, \quad (2.2)$$

are set on the domain boundary and, for $t = 0$, initial condition is given,

$$c(x, 0) = c^0(x). \quad (2.3)$$

From a physical point of view, equation (2.1) can be derived as follows [63]. Consider a two-phase system with component concentrations $c_{1,2}$, $c_1 + c_2 = 1$, and assume that the free energy has a form, with $c = c_1$,

$$\Psi[c, \nabla c] = \int_{\Omega} \psi(c, \nabla c) dx, \quad (2.4)$$

$$\psi(c, \nabla c) = F(c) + \frac{\epsilon^2}{2} |\nabla c|^2, \quad F(c) = c^2(1 - c)^2, \quad (2.5)$$

where ψ is the system free energy density, F is the so-called double-well potential, $\epsilon > 0$ is a small parameter. The first term in (2.5) describes the “dividing” part of the free energy which ensures that the phases do not mix and, hence, the regions with constant $c_{1,2}$ emerge. The second term in (2.5) allows to relate a given energy to the diffuse interface. Parameter ϵ there defines the width of the diffuse interface separating the “pure” phases. Inclusion of the gradient terms makes the system energy depend not only on the quantity of each of the two components but also on the shape of regions taken up by them. Energy form (2.4), (2.5) arises in various models and is typical for weakly non-local (or gradient) thermomechanics.

It should be emphasized that potential $F(c)$ in (2.5) is empirical. Its characteristic feature is the two minima at $c = 0$ and $c = 1$, corresponding to the “pure” phases. The state $c = 1/2$ corresponding to the maximum of $F(c)$ is unstable and, hence, the mixing of the two phases is prevented by the instability. A more accurate and better physically motivated energy model is the so-called logarithmic potential [63]. It possesses essentially the same characteristic properties as the energy form considered here, and the latter can be seen as an approximation of the former.

An illustration of these observations is given in Figure 1. In the left plot, the “separating” part $\psi_{\text{dw}} \equiv F$ of the free energy is shown. The two minima correspond to the “pure” phases, i.e., to the states $c = c_1 = 0$, $c_2 = 1$ and $c = c_1 = 1$, $c_2 = 0$. The state in the neighborhood of $c = 1/2$ is unstable. In the right plot of the figure, a typical stationary solution of the system and energy distribution are shown. As can be seen, the gradient part of the free energy is nonzero only in the diffuse interface regions. At the same time, the separating part of the free energy is zero outside the diffuse interface regions.

Furthermore, one can show that if c is a conservative quantity (as is in our case), the kinetic equation describing the field evolution $c = c(x,t)$ reads [6, 63]:

$$\frac{\partial c}{\partial t} = -\nabla \cdot (-M \nabla \mu), \quad \mu = \frac{\delta \Psi[c, \nabla c]}{\delta c}, \quad (2.6)$$

where $\delta(\cdot)/\delta c$ is the functional derivative (Gateaux derivative). For M constant, due to (2.5), the last relation takes form

$$\frac{1}{M} \frac{\partial c}{\partial t} = \Delta \mu, \quad \mu = -\epsilon^2 \Delta c + F'(c),$$

where Δ is the Laplacian. In the 1D case, under consideration here, this coincides with (2.1).

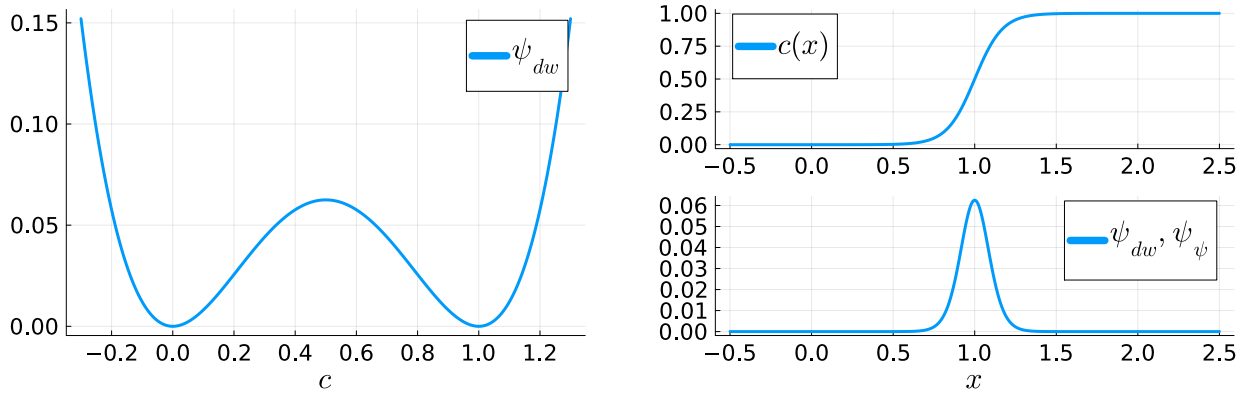


Figure 1: Left: an example of the “separating” free energy part ψ_{dw} . Right: a typical solution and energy distribution.

As can also be shown [12, 63], equation (2.1) has solutions $c = c(x, t)$ with the following fundamental properties:

$$\frac{d}{dt} \int_{\Omega} c = 0, \quad \frac{d}{dt} \Psi[c, \nabla c] \leq 0,$$

which means that c is conserved and the free energy is a non-increasing function of c being the solution of (2.1) or (2.6) and satisfying homogeneous boundary conditions (2.2).

These properties of the analytical solution immediately put restrictions on a numerical scheme for solving (2.1): it should be conservative (which is relatively easy to achieve) and energy-stable, i.e., delivering a discrete analogue of the last inequality (which is more difficult to achieve). In addition, the discrete problem should be uniquely solvable for a given time step size. In practice, this may turn out to be a rather nontrivial task because the potential $F(c)$ is not a convex function and, hence, a discrete solution may be found in a local minimum which is not global and not achievable from an initial state.

3. NUMERICAL ALGORITHMS

This section deals with numerical algorithms applied to solve the Cahn-Hilliard equation. In the first subsection classical time integration schemes are considered, having various degree of implicitness. The second subsection describes the Eyre splitting for the time integration of the Cahn-Hilliard equations. New algorithms based on the LIM scheme are presented in the third subsection.

3.1. Classical time integration schemes

We now consider a number of time integration schemes taking part in the numerical comparisons presented below. All these schemes are well known and described in numerous literature and, in particular, in [64]. All schemes considered in this subsection approximate equation (2.1) and are conservative.

Throughout this paper space derivatives are discretized by finite differences. Assume that a uniform grid with grid size $h = 1/N$ and nodes $x_i = (i - 1/2)h$, $i = \overline{0, N+1}$, with N being the number of grid cells, is used to discretize the equation in the domain Ω . The domain boundaries $x =$

0 and $x = 1$ correspond to points $x_{1/2} = (x_0 + x_1)/2 = 0$ and $x_{N+1/2} = (x_N + x_{N+1})/2 = Nh$ and the grid nodes x_1, x_2, \dots, x_N lie within the domain. For time discretization a uniform grid with time step size τ and nodes $t_n = n\tau$, $n = 0, 1, 2, \dots$, is used. Thus, the solution of the discretized problem is defined in points (x_i, t_j) , $i = 1, N$, $j = 0, 1, \dots$. The corresponding values of the grid functions c_h are denoted by $c_i^n = c(x_i, t_n)$.

Let Δ_h be a standard three-point finite-difference approximation of the Laplacian. In the 1D case under consideration, its values in the nodes $i = 1, N-1$ of the space grid are

$$\Delta_h c_i = \frac{1}{h^2} (c_{i+1} - 2c_i + c_{i-1}).$$

The finite difference equations

$$c_0 - c_1 = 0, \quad c_N - c_{N-1} = 0 \quad (3.1)$$

approximating the homogeneous Neumann boundary conditions (2.2) are related to the boundary nodes $i = 0, N$. Then the resulting discrete Laplacian, with incorporated discretized boundary conditions, is denoted by Δ_h .

Explicit Euler (EE) scheme, the simplest discretization of (2.1), reads

$$\frac{1}{M} \frac{c_i^{n+1} - c_i^n}{\tau} = \Delta_h \mu_i^n, \quad \mu_i^n = F'(c_i^n) - \epsilon^2 \Delta_h c_i^n.$$

The scheme is first order accurate in time and second order accurate in space, is stable for $\tau \sim h^4$ and is not energy stable.

Implicit Euler (IE) scheme reads

$$\frac{1}{M} \frac{c_i^{n+1} - c_i^n}{\tau} = \Delta_h \mu_i^{n+1}, \quad \mu_i^{n+1} = F'(c_i^{n+1}) - \epsilon^2 \Delta_h c_i^{n+1}.$$

The scheme is first order accurate in time and second order accurate in space and is nonlinear (in the sense that a nonlinear equation has to be solved at each time step to determine c_i^{n+1}). It is conditionally (i.e., for a sufficiently small τ) gradient stable and conditionally uniquely solvable, see Table 1.

Crank-Nicolson (CN) scheme can be written as

$$\frac{1}{M} \frac{c_i^{n+1} - c_i^n}{\tau} = \Delta_h \mu_i^{n+1/2}, \quad \mu_i^{n+1/2} = \frac{1}{2} (\mu_i^n + \mu_i^{n+1}),$$

with μ_i^n, μ_i^{n+1} defined above. The scheme is second order accurate in time and second order accurate in space and is nonlinear. It is conditionally gradient stable and conditionally uniquely solvable, see Table 1.

Semi-implicit Euler (SIE) reads

$$\frac{1}{M} \frac{c_i^{n+1} - c_i^n}{\tau} = \Delta_h \mu_i^{n+1}, \quad \mu_i^{n+1} = F'(c_i^n) - \epsilon^2 \Delta_h c_i^{n+1}.$$

The scheme is first order accurate in time and second order accurate in space and is linear. It is unconditionally uniquely solvable and is not energy stable, see Table 1.

3.2. Eyre splitting

The time integration schemes considered up to now are not energy stable and/or not uniquely solvable for arbitrary large time step sizes [12, 13]. An efficient and general way to design time integration schemes, which are both uniquely solvable and energy stable for arbitrary time step sizes, is proposed in papers of David J. Eyre [14, 15]. Since we essentially employ this approach to construct new schemes, we discuss it in more details here.

The essence of the Eyre approach is as follows. The system free energy density ψ , c.f. (2.4), is not a convex function. This is because the dividing part of the free energy is a double-well potential. Assume that ψ can be split as

$$\psi = \psi_c + \psi_e, \quad (3.2)$$

where ψ_c and $-\psi_e$ are *convex* functions. The subindices ‘‘c’’ (meaning ‘‘contraction’’) and ‘‘e’’ (meaning ‘‘expansion’’) reflect their physical meaning. Here the convexity of a function is understood as a positive semi-definiteness of its Hessian, see [13], i.e., a function $f(x)$ is convex provided that $f''(x) \equiv d^2f/dx^2 \geq 0$. Then, the semi-discrete (discrete in time) approximations

$$\frac{1}{M} \frac{c^{n+1} - c^n}{\tau} = \Delta [\mu_c(c^{n+1}) + \mu_e(c^n)], \quad (3.3)$$

with

$$\mu_{c,e} = \frac{\delta \psi_{c,e}}{\delta c}, \quad \mu = \mu_c + \mu_e,$$

are gradient stable and

$$\psi(c^{n+1}) \leq \psi(c^n)$$

holds for any time step size $\tau > 0$. In addition, the convexity of the energy part ψ_c corresponding to the implicitly treated term, ensures the unique solvability of (3.3).

Consider the specific form of the energy functional (2.4). Taking into account that the gradient term in (2.4) belongs to the convex part of the energy, we can take in (3.2)

$$\psi_c = \frac{1}{2} |\nabla c|^2 + F_c, \quad \psi_e = F_e, \quad F_c + F_e = F.$$

Thus, constructing a suitable splitting of the system energy is reduced to splitting the dividing part of the energy F in such a way that

$$F = F_c + F_e, \quad F_c'' \geq 0, \quad -F_e'' \geq 0. \quad (3.4)$$

Then, the chemical potential takes form

$$\mu = \mu_c + \mu_e, \quad \mu_c = -\epsilon^2 \Delta c + F_c', \quad \mu_e = F_e',$$

whereas the semi-discrete system (3.3) can be written as

$$\frac{1}{M} \frac{c^{n+1} - c^n}{\tau} = -\epsilon^2 \Delta^2 c^{n+1} + \Delta F_c'(c^{n+1}) + \Delta F_e'(c^n). \quad (3.5)$$

Splitting of the form (3.4) can be constructed in a number of ways. One of them is to write the dividing part F of the free energy as a sum of two terms according to (3.2). Note that the gradient

part of the free energy (2.5) should be handled together with the convex part ψ_c . Another way is to choose a regularizing function F_r such that

$$F_c = F + F_r, \quad F_e = F - F_r.$$

Although both ways are essentially quite similar, it is convenient to distinguish them due to various possible generalizations.

Consider the specific form (2.5) of F used in this work. We have

$$F(c) = c^2(1 - c^2), \quad F'(c) = 2c(2c^2 - 3c + 1), \quad F''(c) = 2(6c^2 - 6c + 1).$$

Equation $F''(c) = 0$ has roots $c_{1,2} = (3 \pm \sqrt{3})/6$, and, hence, $F''(c) < 0$ for $(3 - \sqrt{3})/6 < c < (3 + \sqrt{3})/6$; $F''(c) \geq 0$ for $c \leq (3 - \sqrt{3})/6$ and $c \geq (3 + \sqrt{3})/6$. Function $F''(c)$ attains its minimum, equal to -1 , at $c = 1/2$. The maxima of $F''(c)$ for $c \in [0,1]$ are attained at $c = 0$ and $c = 1$ and equal 2. Thus, to ensure that F_c and $-F_e$ are convex, it suffices to set

$$F_c = F(c) + \frac{1}{2}c^2, \quad F_e = -\frac{1}{2}c^2.$$

This leads to **non-linearly stabilized splitting scheme (NLSS)**,

$$\frac{1}{M} \frac{c_i^{n+1} - c_i^n}{\tau} = \Delta_h \mu^{n+1}, \quad \mu_i^{n+1} = [F'(c_i^{n+1}) + c_i^{n+1}] - c_i^n - \epsilon^2 \Delta_h c_i^{n+1}. \quad (3.6)$$

The scheme can also be written as

$$\frac{1}{M} \frac{c_i^{n+1} - c_i^n}{\tau} = (\Delta_h - \epsilon^2 \Delta_h^2) c_i^{n+1} + \Delta_h F'(c_i^{n+1}) - \Delta_h c_i^n.$$

It is first order accurate in time, second order in space, implicit, nonlinear in c^{n+1} and energy stable for arbitrary $\tau > 0$.

Another option is to set

$$F_c = c^2, \quad F_e = -c^2 + F(c),$$

which leads to **linearly stabilized splitting scheme (LSS)**,

$$\frac{1}{M} \frac{c_i^{n+1} - c_i^n}{\tau} = \Delta_h \mu_i^{n+1}, \quad \mu_i^{n+1} = 2c_i^{n+1} + [F'(c_i^n) - 2c_i^n] - \epsilon^2 \Delta_h c_i^{n+1}.$$

It may be convenient to write it as

$$\frac{1}{M} \frac{c_i^{n+1} - c_i^n}{\tau} = (2\Delta_h - \epsilon^2 \Delta_h^2) c_i^{n+1} + \Delta_h F'(c_i^n) - 2\Delta_h c_i^n.$$

The scheme is first order accurate in time, second order in space, implicit and, provided that splitting parameters are chosen properly [40], energy stable for arbitrary $\tau > 0$. Unlike the NLSS scheme (3.6), it is linear with respect to c^{n+1} . A three-parameter family of linearly stabilized schemes, including the LSS scheme, is analyzed in [13].

Properties of considered time integration schemes are summarized in Table 1.

Table 1: Properties of time integration schemes according to [12–15, 40] (* provided parameters are chosen properly, see [40]).

Scheme	Linearity	Gradient stability	Solvability
Explicit Euler (EE)	Yes	No	Yes
Implicit Euler (IE)	No	Conditional, $\tau \leq \frac{1}{4}h^2$	$\tau \leq \frac{1}{18}h^2$
Crank-Nicolson (CN)	No	Conditional	$\tau \leq \frac{1}{9}h^2$
Semi-implicit Euler (SIE)	Yes	No	Yes
Nonlinearly stabilized splitting (NLSS)	No	Unconditional	Yes
Linearly stabilized splitting (LSS)	Yes	Unconditional*	Yes

For a fully discrete scheme (i.e., when discretization in time and in space is applied), its gradient stability implies that the free energy functional (2.4) is approximated in a certain way. In this work such an approximation, determined by the space discretization, reads

$$\psi_h(\mathbf{c}) = h \sum_{i=1}^N F'(c_i) + \frac{1}{2}\epsilon^2 h \sum_{i=1}^N \frac{(c_{i+1} - c_i)^2}{h^2}. \quad (3.7)$$

Let a $N \times N$ matrix \mathbf{A} be the matrix of the discussed above discretization $-\Delta_h$ of the operator $-\Delta$, with incorporated homogeneous Neumann boundary conditions (3.1). The space discretization reduces the initial boundary-value problem (2.1)–(2.3) to an initial value problem

$$\frac{1}{M}\mathbf{c}' = -\mathbf{A} \left(F'(\mathbf{c}) + \epsilon^2 \mathbf{A}\mathbf{c} \right), \quad \mathbf{c}(0) = \mathbf{c}^0, \quad (3.8)$$

where the entries of the vector function $\mathbf{c}(t) : \mathbb{R} \rightarrow \mathbb{R}^N$ are the sought after solution values on the space grid and the vector \mathbf{c}^0 contains the grid values of the given function $c^0(x)$.

Let \mathbf{c}^n be an N vector containing the numerical solution values for time level n . Then, the time integration schemes discussed above can be written in a compact form as follows.

- Explicit Euler (EE):

$$\frac{\mathbf{c}^{n+1} - \mathbf{c}^n}{\tau} = -\mathbf{A} \left(F'(\mathbf{c}^n) + \epsilon^2 \mathbf{A}\mathbf{c}^n \right); \quad (3.9)$$

- implicit Euler (IE):

$$\frac{\mathbf{c}^{n+1} - \mathbf{c}^n}{\tau} = -\mathbf{A} \left(F'(\mathbf{c}^{n+1}) + \epsilon^2 \mathbf{A}\mathbf{c}^{n+1} \right); \quad (3.10)$$

- Crank-Nicolson (CN):

$$\frac{\mathbf{c}^{n+1} - \mathbf{c}^n}{\tau} = -\frac{1}{2}\mathbf{A} \left(F'(\mathbf{c}^{n+1}) + \epsilon^2 \mathbf{A}\mathbf{c}^{n+1} + F'(\mathbf{c}^n) + \epsilon^2 \mathbf{A}\mathbf{c}^n \right); \quad (3.11)$$

- Semi-implicit Euler (SIE):

$$\frac{\mathbf{c}^{n+1} - \mathbf{c}^n}{\tau} = -\mathbf{A} \left(F'(\mathbf{c}^n) + \epsilon^2 \mathbf{A}\mathbf{c}^{n+1} \right); \quad (3.12)$$

- nonlinearly stabilized splitting (NLSS)

$$\frac{\mathbf{c}^{n+1} - \mathbf{c}^n}{\tau} = -\mathbf{A} \left(F'(\mathbf{c}^{n+1}) + \mathbf{c}^{n+1} - \mathbf{c}^n + \epsilon^2 \mathbf{A} \mathbf{c}^{n+1} \right); \quad (3.13)$$

- linearly stabilized splitting (LSS)

$$\frac{\mathbf{c}^{n+1} - \mathbf{c}^n}{\tau} = -\mathbf{A} \left(F'(\mathbf{c}^n) - 2\mathbf{c}^n + 2\mathbf{c}^{n+1} + \epsilon^2 \mathbf{A} \mathbf{c}^{n+1} \right). \quad (3.14)$$

We now briefly discuss computational complexity of these schemes. In implicit nonlinear schemes (i.e., IE, CN, NLSS), each time step a nonlinear system of equations has to be solved, e.g., by a Newton iteration. In turn, each Newton iteration involves solving the Jacobian linear system. Implicit linear schemes SIE and LSS require solving a single linear system per time step. Explicit schemes involve neither nonlinear nor linear system solution and have lowest costs per time step. Although implicit time integration schemes allow to use significantly larger time step sizes than explicit schemes, solving large linear systems, within Newton iterations or independently, may become a computationally expensive task. This is because efficiency in sparse direct solvers, as well as in preconditioned iterative solvers, is difficult to retain on modern high-performance hybrid CPU/GPU platforms.

The aim of this work is to develop an efficient numerical algorithm which, on one hand, is gradient stable and allows large time step sizes and, on the other hand, can be efficiently implemented on modern high-performance hybrid platforms. Our approach is based on the combination of the Eyre splitting, in particular the LSS scheme, with the local iteration modified (LIM) scheme. Then, the Eyre splitting allows to use large time step sizes while keeping gradient stability, whereas the LIM mechanism provides a computationally efficient alternative to solving linear systems in implicit schemes.

3.3. Local iteration modified (LIM) scheme

The local iteration modified (LIM) scheme can be viewed as a special explicit scheme where a Chebyshev polynomial of a sufficiently high order p is employed to ensure stability and monotonicity for a given time step size $\tau > 0$. We now describe a LIM variant based on the linearly stabilized splitting (LSS) scheme (3.14), which we write as

$$\mathbf{c}^{n+1} = \left[\mathbf{I} + \tau \widehat{\mathbf{A}} \right]^{-1} \widehat{\mathbf{f}}^n, \quad \widehat{\mathbf{A}} = \mathbf{A} (2\mathbf{I} + \epsilon^2 \mathbf{A}), \quad \widehat{\mathbf{f}}^n = \mathbf{c}^n + \tau \mathbf{A} (2\mathbf{c}^n - F'(\mathbf{c}^n)), \quad (3.15)$$

where \mathbf{I} is the $N \times N$ identity matrix. We emphasize that the inverse matrix here is, of course, never computed, rather a linear system with this matrix is solved. Within the LIM approach the inverse matrix is replaced by a specially chosen Chebyshev polynomial. Let λ_∞ be an upper bound for the largest eigenvalue of $\widehat{\mathbf{A}}$ (in practice one can set $\lambda_\infty := \|\widehat{\mathbf{A}}\|_1 = \max_j \sum_i |\widehat{a}_{ij}|$). The polynomial order p for which stability takes place is chosen as

$$p = \left\lceil \frac{\pi}{4} \sqrt{\tau \lambda_\infty + 1} \right\rceil, \quad (3.16)$$

where $\lceil x \rceil$, for $x \in \mathbb{R}$, denotes the smallest integer greater than or equal to x . Let the Chebyshev polynomial roots

$$\{\beta_m, m = 1, \dots, p\} = \left\{ \cos \pi \frac{2i-1}{2p}, i = 1, \dots, p \right\}$$

be ordered in such a way that no numerical instability occurs for arbitrarily large p and $\beta_1 = \cos(\pi/2p)$ is the first root. We set $z_1 = \beta_1$ and define Chebyshev polynomial parameters

$$a_m = \frac{\lambda_\infty}{1 + z_1} (z_1 - \beta_m), \quad m = 1, \dots, p.$$

Denoting $\mathbf{y}^{(0)} = \mathbf{c}^n$, we obtain the LIM solution \mathbf{c}^{n+1} on the next time level by carrying out $2p - 1$ Chebyshev iterations as

$$\begin{aligned} \mathbf{y}^{(m)} &= \frac{1}{1 + \tau a_m} \left(\mathbf{c}^n + \tau a_m \mathbf{y}^{(m-1)} + \tau (\widehat{\mathbf{f}}^n - \widehat{\mathbf{A}} \mathbf{y}^{(m-1)}) \right), \quad m = 1, \dots, p, \\ \mathbf{y}^{(p+m-1)} &= \frac{1}{1 + \tau a_m} \left(\mathbf{c}^n + \tau a_m \mathbf{y}^{(m-1)} + \tau (\widehat{\mathbf{f}}^n - \widehat{\mathbf{A}} \mathbf{y}^{(m-1)}) \right), \quad m = 2, \dots, p, \\ \mathbf{c}^{n+1} &= \mathbf{y}^{(2p-1)}. \end{aligned} \quad (3.17)$$

Note that $a_1 = 0$ and it is easy to check that the first iteration solution $\mathbf{y}^{(1)}$ is the explicit Euler solution on the next time level. In this sense, the Chebyshev iterations actually start at the second step by computing $\mathbf{y}^{(2)}$. If only the first sweep of iterations is carried out in (3.17), with $\mathbf{y}^{(1)}, \dots, \mathbf{y}^{(p)}$ computed, then setting $\mathbf{c}^{n+1} = \mathbf{y}^{(p)}$ we get a time integration scheme which is known as the regular (non-modified) local iteration scheme (the LI scheme). As already mentioned, in the regular LI scheme stability of the numerical solution is guaranteed for parabolic problems but the solution nonnegativity is not. As one can see, in the LIM scheme (3.17) the second Chebyshev iteration sweep, with $\mathbf{y}^{(p+1)}, \dots, \mathbf{y}^{(2p-1)}$ being computed, the same parameters a_m are employed, except that the first iteration with $a_1 = 0$ (which gives the explicit Euler solution) is not carried out. One can show [58] that formulas (3.17) can be written in an operator form as

$$\mathbf{c}^{n+1} = (\mathbf{I} - \mathbf{F}_p^2) \left[\mathbf{I} + \tau \widehat{\mathbf{A}} \right]^{-1} \widehat{\mathbf{f}}^n, \quad (3.18)$$

where $\widehat{\mathbf{A}}$ and $\widehat{\mathbf{f}}^n$ are defined in (3.15) and \mathbf{F}_p is the Chebyshev polynomial operator,

$$\mathbf{F}_p = \prod_{m=p}^{m=1} \left(\mathbf{I} - \frac{1}{1 + \tau a_m} (\mathbf{I} + \tau \widehat{\mathbf{A}}) \right).$$

By replacing \mathbf{F}_p^2 in (3.18) by \mathbf{F}_p we obtain an operator form of the (regular) LI scheme. Thus, as we see, squaring the Chebyshev polynomial leads to monotonicity in the LIM scheme.

Since scheme (3.17) under consideration is derived from the linearly stabilized splitting (3.14), we call this scheme LIM-LSS. To discover the Eyre splitting effect in this scheme, we include another scheme the numerical experiments presented below. It is obtained by linearizing implicit Euler scheme (3.10). We linearize the scheme by approximating the nonlinear implicit scheme in (3.10) as

$$F'(\mathbf{c}^{n+1}) \approx F'(\mathbf{c}^n) + J_n(\mathbf{c}^{n+1} - \mathbf{c}^n), \quad (3.19)$$

where J_n is the Jacobian of the mapping F' evaluated at \mathbf{c}^n . Substituting approximation (3.19) in (3.10) leads to a linearized implicit Euler (LIE) scheme

$$\mathbf{c}^{n+1} = \left[\mathbf{I} + \tau \widetilde{\mathbf{A}}_n \right]^{-1} \widetilde{\mathbf{f}}^n, \quad \widetilde{\mathbf{A}} = \mathbf{A}(J_n + \epsilon^2 \mathbf{A}), \quad \widetilde{\mathbf{f}}^n = \mathbf{c}^n + \tau \mathbf{A}(J_n \mathbf{c}^n - F'(\mathbf{c}^n)), \quad (3.20)$$

where, just as in scheme (3.15), a linear system solution is understood, so that the inverse matrix is not computed. Comparing schemes (3.15) and (3.20), one can notice that replacing J_n in (3.20) by $2\mathbf{I}$ leads to scheme (3.15).

The LIM scheme based on (3.20) can be obtained in exactly the same as the LIM scheme based on (3.15). One can simply repeat the derivations given above, replacing $\widehat{\mathbf{A}}$ and $\widehat{\mathbf{f}}_n$ by $\widetilde{\mathbf{A}}_n$ and $\widetilde{\mathbf{f}}_n$, respectively. We call the LIM scheme derived in this way the LIM-LIE (LIM linearized implicit Euler) scheme.

A computational efficiency of the LIM schemes can be established, based on the number of required iterations (3.16) and the following reasoning [54, 58]. If the time interval for which the problem has to be solved is increased by a factor s then computational costs of an explicit scheme should also grow by a factor s (as the number of required time steps is s times larger). The same increase in computational costs is also observed if the upper spectral bound λ_∞ is increased by a factor s (since a time step size in an explicit scheme is usually bound to a stability condition of the form $\tau \leq 2/\lambda_\infty$). Recall that for the Cahn-Hilliard equation, in general, we have $\lambda_\infty \sim h^{-4}$. In the LIM schemes the costs grow slower: an increase of the time interval or the upper spectral bound λ_∞ by a factor s leads to an increase in computational work approximately by a factor \sqrt{s} (as the number of required Chebyshev iterations $p \sim (\tau\lambda_\infty)^{1/2}$, see (3.16)). These estimates make clear that the gain in computational costs provided by the LIM schemes increases with the problem size $N = 1/h$ [54, 58]. Nevertheless, it should also be taken into account that the gain actually observed in practice can be restricted by other factors, such as accuracy requirements.

4. COMPUTATIONAL EXPERIMENTS

4.1. Gradient stability tests

In the tests presented here initial-value problem (2.1)–(2.3) is solved for the 1D Cahn-Hilliard equation. Space discretization is done by the standard second order finite differences on a uniform grid, as discussed in the beginning of Section 3.1. This reduces the original initial-boundary value problem to an initial value problem (3.8) to be solved by the time integration schemes (3.9)–(3.13) and new local iteration schemes (3.17) based on (3.14) and (3.20) (the LIM-LSS and LIM-LIE schemes). The parameter ϵ is set to one of the following two values:

$$\epsilon = \epsilon_4(h), \quad \epsilon_m(h) \equiv \frac{hm}{2\sqrt{2} \operatorname{arth}(9/10)}, \quad (4.1)$$

$$\epsilon = \epsilon_4(1/64), \quad (4.2)$$

i.e., ϵ either depends on the space grid size h (formula (4.1), or set to a fixed value $\epsilon = \epsilon_4(1/64)$ of the grid $N = 64$ (formula (4.2)). Note that $m = 4$ in formula (4.1) defines a characteristic number of the grid cells on which a stationary solution changes from its minimum to maximum values.

For all the tested time integration schemes, largest time step sizes for which the gradient stability is observed are reported in Table 2. In these runs, the grid-dependent ϵ values (4.1) are used and a scheme is considered to be gradient stable provided that the discrete energy (3.7) does not increase more than 1% each time step, i.e., for each time step n holds

$$\psi_h(\mathbf{c}^{n+1}) \leq 1.01 \psi_h(\mathbf{c}^n). \quad (4.3)$$

Gradient stability is tested on several initial value vectors \mathbf{c}^0 , where each vector component is taken to be an independent and identically distributed random variable in $[0,1]$, rounded up to the second

Table 2: Largest time step size τ for which time integration schemes are gradient stable, i.e., condition (4.3) holds for $\epsilon = \epsilon_4(h)$

h	1/32	1/64	1/128	1/256
EE	8.8×10^{-5}	2.1×10^{-5}	5.4×10^{-6}	1.3×10^{-6}
IE	5.1×10^{-3}	1.3×10^{-3}	3.0×10^{-4}	8.1×10^{-5}
CN	2.4×10^{-3}	6.8×10^{-4}	1.7×10^{-4}	3.8×10^{-5}
SIE	2.2×10^{-3}	5.7×10^{-4}	1.9×10^{-4}	4.0×10^{-5}
LSS	∞	∞	∞	∞
NLSS	∞	∞	∞	∞
LIM-LSS	∞	∞	∞	∞
LIM-LIE	9.9×10^{-3}	2.8×10^{-3}	5.8×10^{-4}	1.2×10^{-4}
LIE	5.8×10^{-3}	1.6×10^{-3}	3.2×10^{-4}	8.3×10^{-5}

digit after the decimal point. Table 2 also contains results for the linearized implicit Euler (LIE) scheme (3.20).

As can be seen in the table, only Eyre splitting based schemes turn out to be unconditionally gradient stable. In the tests, a scheme is considered to be unconditionally gradient stable if gradient stability is observed for $\tau \leq 500$. Furthermore, we note that maximum time step size in the implicit scheme exceeds the maximum time step size in the explicit schemes approximately by the same factor (≈ 60) for all h . Comparing the LIE and IE schemes, we see that linearization does not corrupt the gradient stability of the implicit scheme. The LIM-LSS scheme conserves the unconditional gradient stability of the LSS scheme, and the LIM-LIE scheme inherits the conditional gradient stability of the LIE scheme. One of the aims of this work is to show that implicit schemes can be successfully replaced by stable explicit schemes. Having this in mind, we may conclude from Table 2 that both LIM schemes work well. This, of course, does imply that increasing the time step size τ in both LIM-LSS and LIM-LIE schemes leads to an increase of the Chebyshev iterations required per time step. We also note that the values presented in our Table 2 are close to the values reported in Table 1 from paper [64].

4.2. Accuracy and efficiency tests

The tests discussed here are aimed to evaluate accuracy and computational efficiency of the considered schemes and, in particular, to discover whether the LIM schemes provide a gain in computational costs with respect to the explicit Euler (EE) scheme. Since the costs per time step in the EE scheme are minimal, it is clear that other time integration schemes can deliver a higher computational efficiency only if the time step size is increased. However, increasing the time step size is possible only provided the delivered numerical accuracy remains within the allowed tolerance. We estimate accuracy of a time integration scheme by comparing its solution at the final time $t = T$ to the reference solution $\mathbf{c}_{\text{ref}}(T)$, which is computed for each space grid with a tiny time step size $\tau = 10^{-9}$. The initial value vector is set to have random entries, in the same way as in the previous tests, then fixed and used for a current space grid in all time integration schemes. For each scheme

Table 3: The upper spectral bound $\lambda_\infty = \|\widehat{\mathbf{A}}\|_1$ for the LIM-LSS scheme and the maximum time step size τ_{\max} , for which the EE scheme is gradient stable (row 3 in the table) and the LIM-LSS scheme operates in the explicit scheme mode (rows 4 and 6), depending on h . As seen in the table, $\lambda_\infty = O(h^{-2})$ for $\epsilon = \epsilon_4(h)$, $\lambda_\infty = O(h^{-4})$ for $\epsilon = \epsilon_4(1/64)$ and in all cases $\tau_{\max} = O(\lambda_\infty^{-1})$.

h	1/32	1/64	1/128	1/256	1/512
		$\epsilon = \epsilon_4(h)$			
$\lambda_\infty = \ \widehat{\mathbf{A}}\ _1$	2.3×10^4	9.3×10^4	3.7×10^5	1.5×10^6	6.0×10^6
gradient stability	8.8×10^{-5}	2.1×10^{-5}	5.4×10^{-6}	1.3×10^{-6}	3.3×10^{-7}
explicit scheme mode	2.6×10^{-5}	6.6×10^{-6}	1.6×10^{-6}	4.1×10^{-7}	1.0×10^{-7}
		$\epsilon = \epsilon_4(1/64)$			
$\lambda_\infty = \ \widehat{\mathbf{A}}\ _1$	1.2×10^4	9.3×10^4	1.1×10^6	1.6×10^7	2.5×10^8
explicit scheme mode	5.1×10^{-5}	6.6×10^{-6}	5.6×10^{-7}	3.8×10^{-8}	2.4×10^{-9}

the achieved accuracy is measured as a relative error norm

$$\frac{\|\mathbf{c}^n - \mathbf{c}_{\text{ref}}(T)\|}{\|\mathbf{c}_{\text{ref}}(T)\|}, \quad n = n_{\text{final}} = T/\tau, \quad (4.4)$$

where $\|\mathbf{c}\| = \sqrt{\mathbf{c}^T \mathbf{c}}$ is the Euclidean vector norm.

In all tests we set the final time T equal to $T = 0.2$. At this T the solution has already passed the initial phase of forming homogeneous regions for times $t \approx \epsilon^2$, all the schemes need sufficiently many time steps, but the solution is still far from its stationary state.

Table 3 presents the values of the upper spectral bound λ_∞ depending on the grid step h and the corresponding maximum time step size values τ at which the explicit scheme is stable. In each case, two maximum τ values are given in the table:

(a) a maximum time step size τ , for which gradient stability is observed (i.e., no energy increase (4.3) takes place); (b) a maximum time step size τ , for which the schemes LIM-LIE and LIM-LSS operate in the explicit scheme mode, i.e., for which relation (3.16) yields $p = 1$, meaning that no Chebyshev iterations are needed.

The last condition implies that the EE scheme is stable in the Euclidean operator norm. This can be seen from the following. If for the LIM-LIE scheme relation (3.16) gives $p = 1$ then

$$\tau \lambda_\infty \leq \left(\frac{4}{\pi}\right)^2 - 1, \quad (4.5)$$

where $\lambda_\infty = \|\widetilde{\mathbf{A}}\|_1$ with $\widetilde{\mathbf{A}}$ being defined in (3.20). If $J_n = \partial F'(\mathbf{c}^n)/\partial \mathbf{c}$ then, taking into account approximation $F'(\mathbf{c}^n) \approx F'(\mathbf{0}) + J_n(\mathbf{c}^n - \mathbf{0}) = J_n \mathbf{c}^n$, we obtain, for the EE solution \mathbf{c}^{n+1} ,

$$\|\mathbf{c}^{n+1}\| = \|\mathbf{c}^n - \tau \mathbf{A}(F'(\mathbf{c}^n) + \epsilon^2 \mathbf{A} \mathbf{c}^n)\| \approx \|(I - \tau \widetilde{\mathbf{A}}) \mathbf{c}^n\| \leq \|I - \tau \widetilde{\mathbf{A}}\| \|\mathbf{c}^n\|.$$

Since $\widetilde{\mathbf{A}}$ is symmetric positive semidefinite matrix, condition $\|I - \tau \widetilde{\mathbf{A}}\|_2 \leq 1$ in the Euclidean operator norm is equivalent to $\tau \|\widetilde{\mathbf{A}}\|_2 \leq 2$, which follows from (4.5) (note that $\|\widetilde{\mathbf{A}}\|_2 \leq \|\widetilde{\mathbf{A}}\|_1 = \lambda_\infty$).

Table 3 shows dependence of the upper spectral bound λ_∞ on h for the LIM-LSS scheme, i.e., $\lambda_\infty = \|\widehat{\mathbf{A}}\|_1$. In the tests presented here in all cases the values of $\|\widehat{\mathbf{A}}\|_1$ and $\|\widetilde{\mathbf{A}}\|_1$ appear to be so

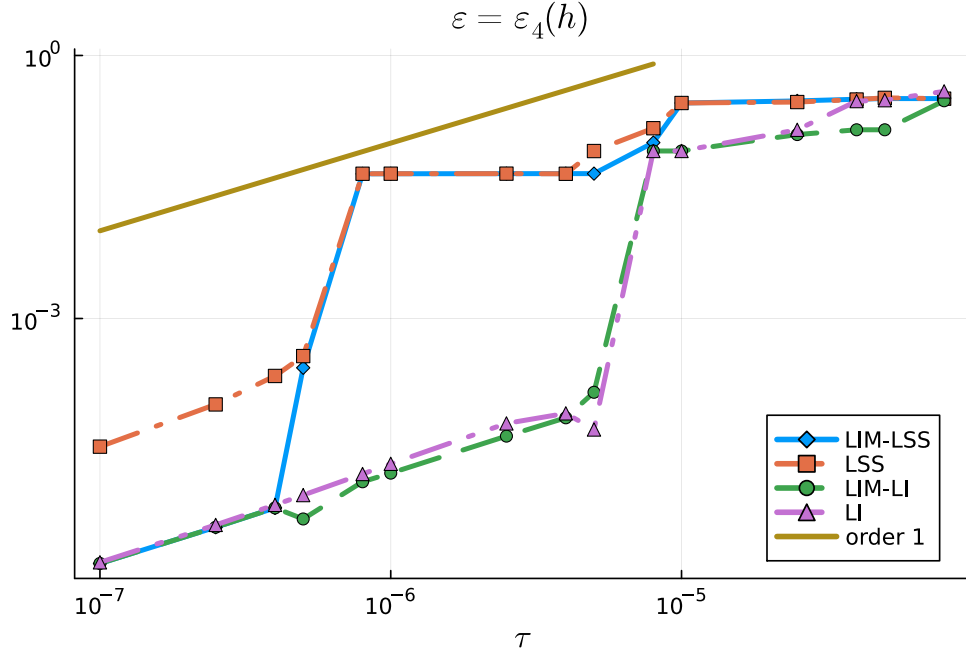


Figure 2: Convergence (achieved accuracy versus the time step size τ) for the LIM-LSS, LSS, LIM-LIE and LI schemes on the $N = 256$ space grid, $\epsilon = \epsilon_4(h)$

close that the Chebyshev iteration numbers in the LIM-LSS and LIM-LIE schemes turn out to be almost the same. The values in Table 3 are given for the both ways to determine ϵ , see (4.1), (4.2). From the table data, it is easy to check that for the choice $\epsilon = \epsilon_4(h)$ the matrix $\epsilon^2 \mathbf{A}$ does not depend on h . Hence, taking into account (3.15), we obtain a dependence $\|\hat{\mathbf{A}}\|_1 = \mathcal{O}(h^{-2})$. For ϵ defined in the second way (by formula (4.2)), we have $\|\hat{\mathbf{A}}\|_1 = \mathcal{O}(h^{-4})$.

The first order convergence $\mathcal{O}(\tau)$ of the schemes LIM-LSS, LSS, LIM-LIE and LI is confirmed by the plot in Figure 2. As can be seen from the figure, both LIM schemes retain the accuracy properties of the schemes they are based on. In addition, we note that the Eyre splitting schemes LSS and LIM-LSS turn out to be less accurate than the LIM-LIE and LI schemes. In the former, the gradient stability is achieved by the splitting, which leads to an additional error.

In Tables 4–7 computational costs and achieved accuracies, depending on the time step size τ , are given for the EE, LSS, LIM-LSS, and LIM-LIE schemes. As we see in tables, accuracies delivered by the LSS and LIM-LSS schemes turn out to be too low (we consider error values (4.4) greater than 10^{-2} unacceptably large). In these schemes, a time step size increase with respect to the EE scheme, needed to compensate higher costs per time step, leads to an unacceptably low accuracy. The LIM-LIE scheme is more accurate and yields a gain with respect to the EE scheme on fine grids (the gain is approximately a factor 2 on the $N = 512$ grid). The fact that the low accuracy of the LSS and LIM-LSS is caused by the Eyre splitting, is confirmed by switching to the LI and LIM-LIE schemes (the LI scheme error values are not shown in the table, they are close to that of the LIM-LIE scheme, see Figure 2).

Plots showing achieved accuracy versus computational costs are given in Figure 3. As can be seen in the plots, the LIM schemes perform better on the $N = 512$ grid than on the $N = 256$ grid: a cost reduction of an approximately factor 3 is achieved on the $N = 512$ grid.

In the presented tests a rather low achieved accuracy is observed for all the schemes except the

Table 4: Number of matrix-vector multiplications (matvecs), number of linear system solutions (for implicit schemes LSS and LIE), and achieved accuracy versus τ . $\epsilon = \epsilon_4(h)$, space grid $N = 64$

τ	scheme	# matvecs / # lin.syst. solutions $\times 10^3$	error (4.4)
5.0×10^{-5}	LIM-LSS	12 / —	5.24×10^{-2}
	LSS	4 / 4	1.18×10^{-1}
	LIM-LIE	12 / —	8.34×10^{-3}
1.0×10^{-5}	EE	20 / —	1.04×10^{-4}
	LIM-LSS	60 / —	2.52×10^{-2}
	LSS	20 / 20	2.92×10^{-2}
	LIM-LIE	60 / —	3.96×10^{-4}
1.0×10^{-6}	EE	200 / —	2.27×10^{-5}
	LIM-LSS	200 / —	2.27×10^{-5}
	LSS	200 / 200	2.93×10^{-3}
	LIM-LIE	200 / —	2.27×10^{-5}

Table 5: Number of matrix-vector multiplications (matvecs), number of linear system solutions (for implicit schemes LSS and LIE), and achieved accuracy versus τ . $\epsilon = \epsilon_4(h)$, space grid $N = 128$.

τ	scheme	# matvecs / # lin.syst. solutions $\times 10^3$	error (4.4)
2.5×10^{-5}	LIM-LSS	40 / —	1.71×10^{-1}
	LSS	8 / 8	1.66×10^{-1}
	LIM-LIE	40 / —	9.06×10^{-2}
5.0×10^{-6}	EE	40 / —	3.37×10^{-4}
	LIM-LSS	120 / —	3.60×10^{-2}
	LSS	40 / 40	1.19×10^{-2}
	LIM-LIE	120 / —	7.91×10^{-4}

Table 6: Number of matrix-vector multiplications (matvecs), number of linear system solutions (for implicit schemes LSS and LIE), and achieved accuracy versus τ . $\epsilon = \epsilon_4(h)$, space grid $N = 256$.

τ	scheme	# matvecs / # lin.syst. solutions $\times 10^3$	error (4.4)
1.0×10^{-5}	LIM-LIE	140 / —	8.14×10^{-2}
5.0×10^{-6}	LIM-LSS	200 / —	4.49×10^{-2}
	LSS	40 / 40	8.12×10^{-2}
	LIM-LIE	200 / —	1.44×10^{-4}
1.0×10^{-6}	EE	200 / —	2.06×10^{-5}
	LIM-LSS	600 / —	4.48×10^{-2}
	LSS	200 / 200	4.48×10^{-2}
	LIM-LIE	600 / —	1.72×10^{-5}

Table 7: Number of matrix-vector multiplications (matvecs), number of linear system solutions (for implicit schemes LSS and LIE), and achieved accuracy versus τ , $\epsilon = \epsilon_4(h)$, space grid $N = 512$.

τ	scheme	# matvecs / # lin.syst. solutions $\times 10^6$	error (4.4)
2.0×10^{-6}	LIM-LIE	0.5 / —	8.25×10^{-6}
1.0×10^{-6}	LIM-LSS	1 / —	3.25×10^{-2}
	LSS	0.2 / 0.2	3.25×10^{-2}
	LIM-LIE	1 / —	4.61×10^{-6}
2.0×10^{-7}	EE	1 / —	9.57×10^{-7}
	LIM-LSS	3 / —	3.25×10^{-2}
	LSS	1 / 1	3.25×10^{-2}
	LIM-LIE	3 / —	7.35×10^{-7}

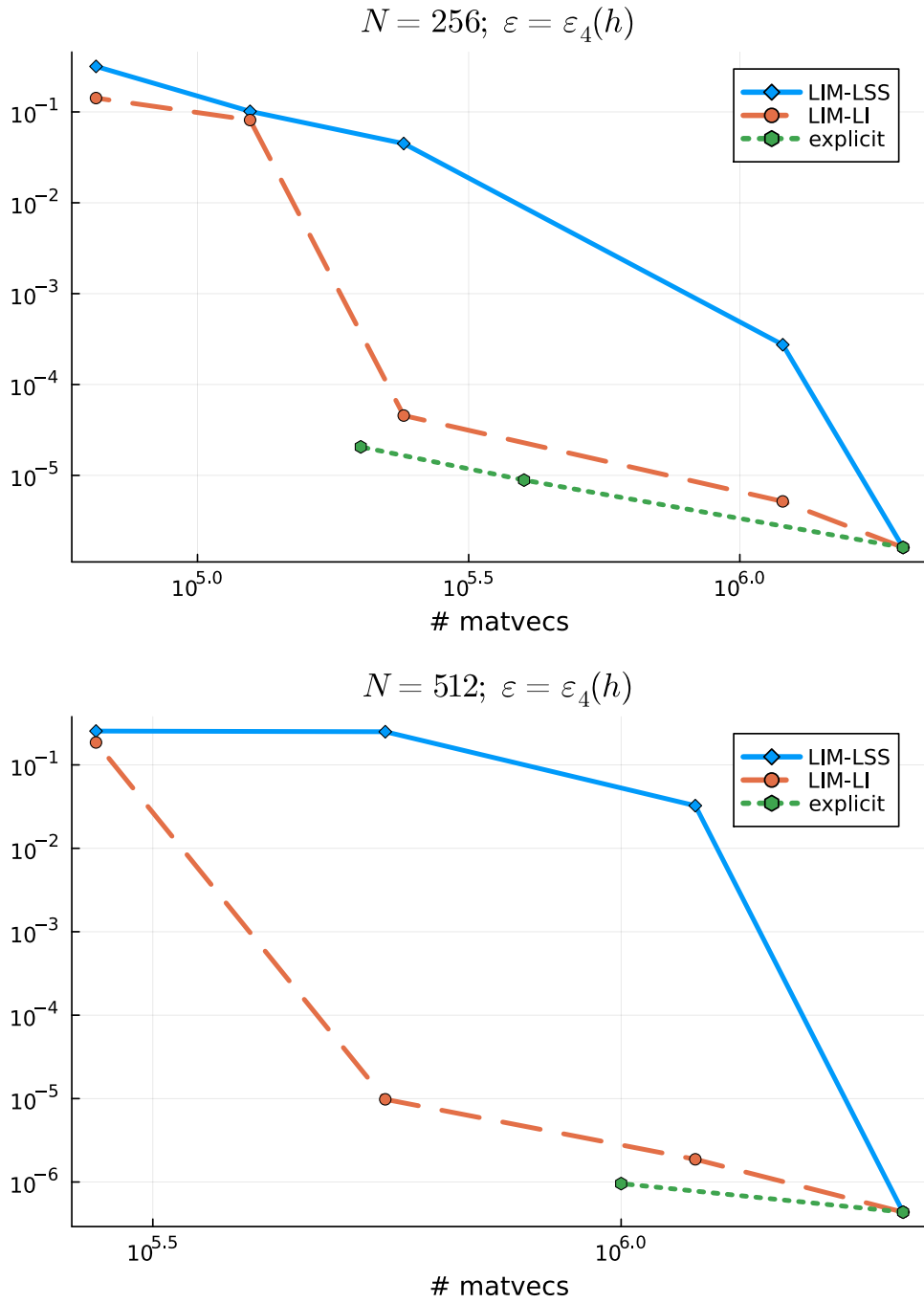


Figure 3: Achieved accuracy versus number of matrix-vector multiplications (matvecs) for the EE and LIM schemes on the $N = 256$ space grid (upper plot) and $N = 512$ space grid (lower plot), $\epsilon = \epsilon_4(h)$. Increasing τ in the EE scheme further is impossible due to the stability restrictions.

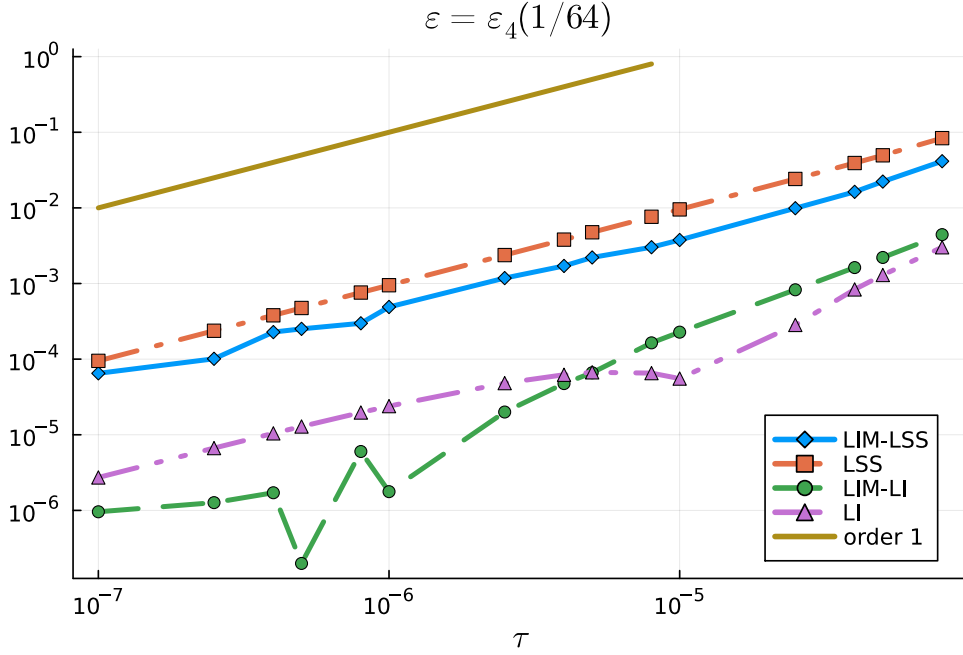


Figure 4: Convergence (achieved accuracy versus the time step size τ) for the LIM-LSS, LSS, LIM-LIE and LIE schemes on the $N = 256$ space grid, $\epsilon = \epsilon_4(1/64)$

EE scheme and this is not only due to the Eyre splitting. In our tests the initial value vector is a non-smooth grid function, where each vector entry is chosen randomly. As discussed above in the introduction, a fast forming of the homogeneity regions is observed for such initial values, taking place at typical evolution times ϵ^2 . Hence, to properly track this process, the time step size should be chosen as $\tau \sim \mathcal{O}(\epsilon^2) = \mathcal{O}(h^2)$. Therefore, taking into account that $\epsilon^2 \|A\| \sim \epsilon^2 h^{-2} = \mathcal{O}(1)$, we see that during this initial phase of the time integration the time step size τ can not be taken much larger than the time step size in the EE scheme. This time step is, in this case, determined by the accuracy rather than by the stability requirements.

To test the stability and accuracy of the considered time integration schemes at larger time steps, we carry out tests with a smoother initial condition. For the space grids $N > 64$, we set it by interpolating the initial non-smooth initial solution from the grid $N = 64$ to the current (finer) space grid. On the $N = 64$ space grid the initial vector does not change. The interpolation is done by the piecewise cubic Hermite interpolation, which excludes the occurrence of new extrema and yields a continuously differentiable function (in the octave package, this interpolation method is called `pchip`). In addition, in the tests with the smoothed initial value vector, the second method (4.2) for setting ϵ is employed, which allows to test our schemes in the situation when the norm of the right-hand side operator grows as $\mathcal{O}(h^{-4})$, see Table 3.

We start by testing the first order convergence $\mathcal{O}(\tau)$ at the plot in Figure 4. Comparing the plot with the plot in 2, we see that all the schemes achieve a much higher accuracy. However, the LSS and LIM-LSS schemes based on the Eyre splitting are still less accurate than the LIE and LIM-LIE schemes. Small error oscillations observed with the LIM-LIE scheme for $\tau \approx 10^{-6}$ are caused by the fact that number of Chebyshev iterations carried out each time step slightly varies for these τ values.

Test results for smoothed initial value vectors and fixed $\epsilon = \epsilon_4(1/64)$ are presented in Tables 8–10 and in Figure 5. We see that both LIM schemes provide an essential efficiency gain with respect

Table 8: Number of matrix-vector multiplications (matvecs), number of linear system solutions (for implicit schemes LSS and LIE), and achieved accuracy versus τ . $\epsilon = \epsilon_4(h)$, smoothed initial vector \mathbf{c}^0 , space grid $N = 128$.

τ	scheme	# matvecs / # lin.syst. solutions $\times 10^3$	error (4.4)
1.0×10^{-4}	LIM-LSS	34 / —	7.46×10^{-2}
	LSS	2 / 2	1.37×10^{-1}
	LIM-LIE	34 / —	6.06×10^{-3}
5.0×10^{-6}	LIM-LSS	200 / —	3.42×10^{-3}
	LSS	40 / 40	5.25×10^{-3}
	LIM-LIE	185 / —	1.09×10^{-4}
1.0×10^{-6}	EE	200 / —	3.02×10^{-5}
	LIM-LSS	600 / —	8.14×10^{-4}
	LSS	200 / 200	1.04×10^{-3}
	LIM-LIE	600 / —	1.50×10^{-5}

to the EE scheme. On the $N = 512$ grid the gain of approximately a factor 10 is attained (see the bottom plot in Figure 5).

5. CONCLUSIONS

The presented results allow to make the following conclusions.

- 1) Proposed local iteration schemes LIM-LSS and LIM-LIE (3.17), which are based on the implicit schemes LSS (3.14) and LIE (3.20), proved to be reliable in practice. They combine a simplicity and parallelism of explicit schemes with stability of implicit schemes. Theoretical estimates of efficiency for the LIM schemes are confirmed in the tests: the LIM schemes provide an efficiency gain up to a factor 10 with respect to the explicit scheme EE. The gain factor grows as the space grid gets finer.
- 2) In the considered numerical tests, gradient stable schemes based on the Eyre splitting appear to be less accurate than regular linearized schemes. In particular, the regular linearized implicit Euler scheme LIE (3.20) and based on it local iteration scheme LIM-LIE provide a higher accuracy than the linear stabilized splitting scheme LSS (3.14) and the local iteration scheme LIM-LSS. In the latter schemes a gradient stability is achieved by splitting, which leads to an additional error.
- 3) In cases where the diffusion boundary width ϵ is chosen proportional to the grid size, i.e., $\epsilon = \mathcal{O}(h)$, the time step size in the explicit scheme EE is bounded as $\tau = \mathcal{O}(h^2)$. Therefore, we can expect that the potential of the local iteration schemes for the Cahn-Hilliard equation is comparable to that for parabolic problems.
- 4) For non-smooth initial data, for instance, if the initial value vector is chosen randomly, additional accuracy restrictions on the time step size τ arise at times $t \leq \mathcal{O}(\epsilon^2)$. Since decreasing

Table 9: Number of matrix-vector multiplications (matvecs), number of linear system solutions (for implicit schemes LSS and LIE), and achieved accuracy versus τ . $\epsilon = \epsilon_4(h)$, smoothed initial vector \mathbf{c}^0 , space grid $N = 256$.

τ	scheme	# matvecs / # lin.syst. solutions $\times 10^6$	error (4.4)
1.0×10^{-5}	LIM-LSS	0.38 / —	3.76×10^{-3}
	LSS	0.02 / 0.02	9.55×10^{-3}
	LIM-LIE	0.38 / —	2.27×10^{-4}
5.0×10^{-7}	LIM-LSS	2 / —	2.51×10^{-4}
	LSS	0.4 / 0.4	4.75×10^{-4}
	LIM-LIE	2 / —	1.99×10^{-7}
1.0×10^{-7}	EE	2 / —	2.76×10^{-6}
	LIM-LSS	6 / —	6.49×10^{-5}
	LSS	2 / 2	9.49×10^{-5}
	LIM-LIE	6 / —	9.59×10^{-7}

Table 10: Number of matrix-vector multiplications (matvecs), number of linear system solutions (for implicit schemes LSS and LIE), and achieved accuracy versus τ . $\epsilon = \epsilon_4(h)$, smoothed initial vector \mathbf{c}^0 , space grid $N = 512$.

τ	scheme	# matvecs / # lin.syst. solutions $\times 10^6$	error (4.4)
8.0×10^{-7}	LIM-LSS	5.75 / —	3.14×10^{-4}
	LSS	0.25 / 0.25	7.13×10^{-4}
	LIM-LIE	5.75 / —	3.83×10^{-6}
4.0×10^{-8}	LIM-LSS	25 / —	1.65×10^{-5}
	LSS	5 / 5	3.56×10^{-5}
	LIM-LIE	25 / —	9.87×10^{-8}
8.0×10^{-9}	EE	25 / —	1.98×10^{-7}
	LIM-LSS	75 / —	4.44×10^{-6}
	LSS	25 / 25	7.13×10^{-6}
	LIM-LIE	75 / —	5.14×10^{-8}

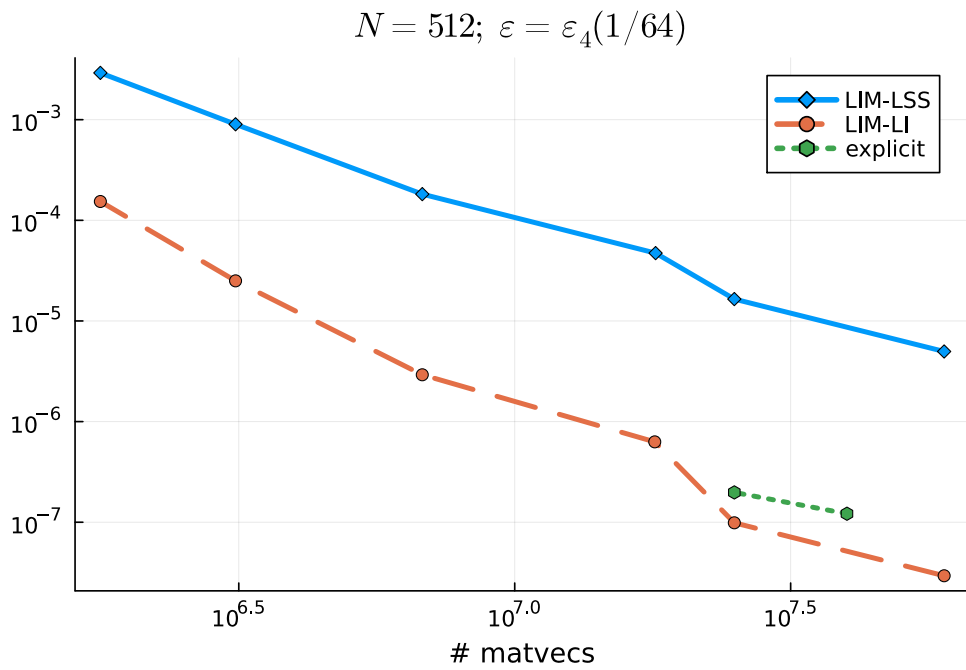
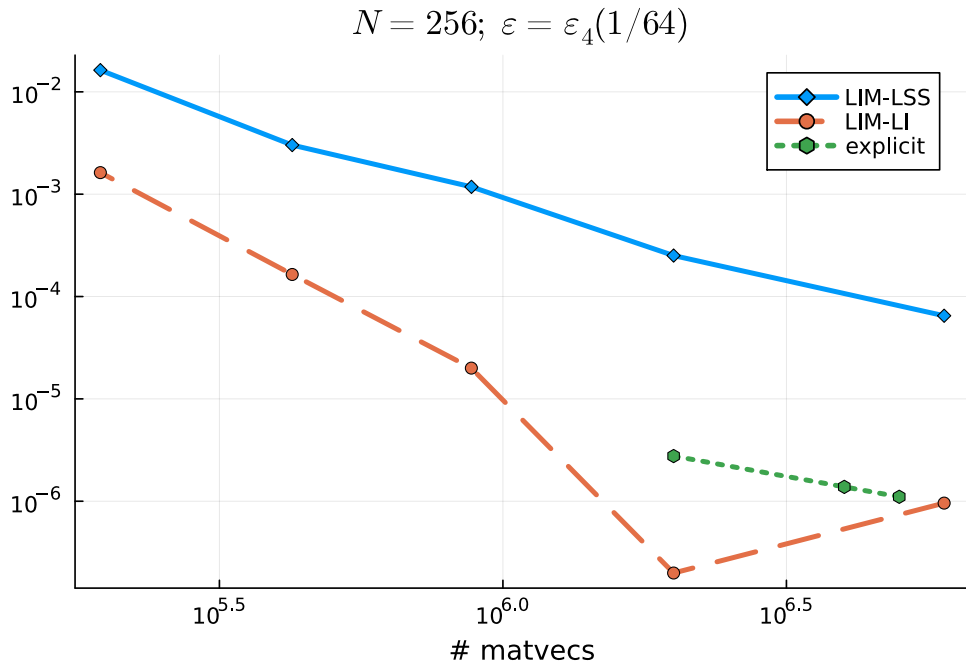


Figure 5: Achieved accuracy versus the number of matrix-vector multiplications (matvecs) for the EE scheme and the LIM schemes with the smoothed initial vector \mathbf{c}^0 and $\varepsilon = \varepsilon_4(1/64)$ on the $N = 256$ grid (upper plot) and the $N = 512$ grid (bottom plot). Increasing τ in the EE scheme further is impossible due to the stability restrictions.

the time step size in an implicit scheme usually means lowering its efficiency, the local iteration schemes appear to be especially attractive (in these schemes decreasing the time step size does lead to lower computational costs). In such problems it seems sensible to apply local iterations schemes with an adaptive choice of the time step size [65].

Acknowledgments

The authors thank V.T. Zhukov (KIAM RAS) for useful discussions and consulting on local iterations schemes.

REFERENCES

1. *Cahn, J.W., Hilliard, J.E.* Free Energy of a Nonuniform System. I. Interfacial Free Energy // The Journal of Chemical Physics. 1958. V. 28. № 2. pp. 258-267. <https://doi.org/10.1063/1.1744102>
2. *Gurtin, M.E.* Generalized Ginzburg-Landau and Cahn-Hilliard equations based on a microforce balance // Physica D: Nonlinear Phenomena. 1996. V. 92. Iss. 3–4., pp. 178-192. [https://doi.org/10.1016/0167-2789\(95\)00173-5](https://doi.org/10.1016/0167-2789(95)00173-5)
3. *Provatas, N., Elder, K.* Phase-Field Methods in Materials Science and Engineering. First published: 7 October 2010 DOI:10.1002/9783527631520. 2010 Wiley-VCH Verlag GmbH & Co. KGaA
4. *Steinbach, I., Salama, H.* Lectures on Phase Field. Springer Cham, 2023. <https://doi.org/10.1007/978-3-031-21171-3>
5. *Skripov V P, Skripov A V* “Spinodal decomposition (phase transitions via unstable states)” Sov. Phys. Usp. 22 389–410 (1979) <https://doi.org/10.3367/UFNr.0128.197906a.0193>
6. *Hohenberg, P.C., Halperin, B.I.* Theory of dynamic critical phenomena // Rev. Mod. Phys. 177. V. 49. Iss. 3. pp. 435. <https://doi.org/10.1103/RevModPhys.49.435>
7. *Penrose, O., Fife, P.C.* Thermodynamically consistent models of phase-field type for the kinetic of phase transitions // Physica D: Nonlinear Phenomena. 1990. V. 43. Iss. 1. pp. 44-62. [https://doi.org/10.1016/0167-2789\(90\)90015-H](https://doi.org/10.1016/0167-2789(90)90015-H).
8. *Bray, A.J.* Theory of phase-ordering kinetics // Advances in Physics. 2002. V. 51, № 2. pp. 481-587. <https://doi.org/10.1080/00018730110117433>
9. *Miranville, A.* The Cahn–Hilliard Equation: Recent Advances and Applications // Society for Industrial and Applied Mathematics. 2019. <https://doi.org/10.1137/1.9781611975925>
10. *Pego, R.L.* Front Migration in the Nonlinear Cahn-Hilliard Equation // Proceedings of the Royal Society of London. Series A, Mathematical and Physical Sciences. 1989. V. 422, No. 863. pp. 261-278. <http://www.jstor.org/stable/2398477>
11. *Bates, P.W., Fife, P.C.* The Dynamics of Nucleation for the Cahn-Hilliard Equation // SIAM Journal on Applied Mathematics. 1993. V. 53. No. 4. pp. 990–1008. <http://www.jstor.org/stable/2102259>.
12. *de Mello, E.V.L., Otton Teixeira da Silveira Filho* Numerical study of the Cahn–Hilliard equation in one, two and three dimensions // Physica A: Statistical Mechanics and its Applications. 2005. V. 347. pp. 429-443, <https://doi.org/10.1016/j.physa.2004.08.076>
13. *Vollmayr-Lee, B.P., Rutenberg, A.D.* Fast and accurate coarsening simulation with an unconditionally stable time step // Phys. Rev. E. 2003. V. 68. Iss. 6. p. 066703. <https://doi.org/10.1103/PhysRevE.68.066703>

14. *Eyre, D.J.* An unconditionally stable one-step scheme for gradient systems // Tech. report, Department of Mathematics, University of Utah. 1997. unpublished. <https://api.semanticscholar.org/CorpusID:117273508>
15. *Eyre, D.J.* Unconditionally gradient stable time marching the Cahn-Hilliard equation // Computational and Mathematical Models of Microstructural Evolution, Mater. Res. Soc. Symp. Proc., ed., vol. 529, Bullard, J.W. and Chen, L.-Q. and Kalia, R.K. and Stoneham, A.M., 1998, pp. 39–46.
16. *Tierra, G., Guillén-González, F.* Numerical methods for solving the Cahn-Hilliard equation and its applicability to related Energy-based models // Nečas Center for Mathematical Modeling, Preprint no. 2013-035.
17. *Cueto-Felgueroso, L., Peirraire, J.* A time-adaptive finite volume method for the Cahn–Hilliard and Kuramoto–Sivashinsky equations // J. Comput. Phys. 2008. V. 227. Iss. 4. pp. 9985–10017. <https://doi.org/10.1016/j.jcp.2008.07.024>
18. *Li, Y., Choi, Y., Kim, J.* Computationally efficient adaptive time step method for the Cahn–Hilliard equation // Computers & Mathematics with Applications. 2017. V. 73. Iss. 8. pp. 1855-1864. <https://doi.org/10.1016/j.camwa.2017.02.021>
19. *Zhang, Z., Qiao, Z.* An Adaptive Time-Stepping Strategy for the Cahn-Hilliard Equation // Communications in Computational Physics. 2012. V. 11. Iss.4. pp. 1261-1278. <https://doi.org/10.4208/cicp.300810.140411s>
20. *Minkoff, S. E., Kridler, N. M.* A comparison of adaptive time stepping methods for coupled flow and deformation modeling // Appl. Math. Model. 2006. V. 30. Iss. 9. pp. 993–1009. <https://doi.org/10.1016/j.apm.2005.08.002>
21. *Luo, F., Tang, T., Xie, H.* Parameter-Free Time Adaptivity Based on Energy Evolution for the Cahn-Hilliard Equation // Communications in Computational Physics. 2016. V. 19., Iss. 5. pp. 1542-1563. <https://doi.org/10.4208/cicp.scpde14.45s>
22. *Guillén-González, F., Tierra, G.* Second order schemes and time-step adaptivity for Allen-Cahn and Cahn-Hilliard models // Computers and Mathematics with Applications. 2014. V. 68. Iss. 8. pp. 821–846. <https://doi.org/10.1016/j.camwa.2014.07.014>
23. *Kassam, A., Trefethen, L.*, Fourth-order time-stepping for stiff PDEs // SIAM J. Sci. Comput. 2005. V. 26. Iss. 4. pp. 1214–1233. <https://doi.org/10.1137/S1064827502410633>
24. *He, Y., Liu, Y., Tang, T.* On large time-stepping methods for the Cahn–Hilliard equation // Applied Numerical Mathematics. 2007. V. 57. Iss. 5–7. pp. 616-628. <https://doi.org/10.1016/j.apnum.2006.07.026>
25. *Song, H.* Energy stable and large time-stepping methods for the Cahn–Hilliard equation // International Journal of Computer Mathematics. 2015. V. 92. Iss. 10. pp. 2091-2108. <https://doi.org/10.1080/00207160.2014.964694>
26. *Li, D.* Why large time-stepping methods for the Cahn-Hilliard equation is stable // Math. Comp. 2022. V. 91. № 238. pp. 2501-2515. <https://doi.org/10.1090/mcom/3768>

27. *Chen, W., Wang, C., Wang, X., Wise, S.M.* Positivity-preserving, energy stable numerical schemes for the Cahn-Hilliard equation with logarithmic potential // *Journal of Computational Physics*: X. 2009. V. 3. pp. 100031, <https://doi.org/10.1016/j.jcp.2019.100031>
28. *Chen, W., Wang, X., Yan, Y., Zhang, Z.* A Second Order BDF Numerical Scheme with Variable Steps for the Cahn-Hilliard Equation // *SIAM Journal on Numerical Analysis*. 2019. V. 57. Iss. 1. pp. 495-525. <https://doi.org/10.1137/18M1206084>
29. *Zhang, J., Jiang, M., Gong, Y., & Zhao, J.* Energy-stable predictor-corrector schemes for the Cahn-Hilliard equation // *J. Comput. Appl. Math.* 2020. V. 376. pp. 112832. <https://doi.org/10.1016/j.cam.2020.112832>
30. *Zhou, Q., Sun, Y.* Energy stability of exponential time differencing schemes for the nonlocal Cahn-Hilliard equation // *Numer. Methods Partial Differ. Eq.* 2023. V. 39. Iss. 5. pp. 4030–4058. <https://doi.org/10.1002/num.23035>
31. *Lee, S.* Unconditionally strong energy stable scheme for Cahn–Hilliard equation with second-order temporal accuracy // *Math Meth Appl Sci.* 2023. V. 46. Iss. 6. pp. 6463-6469. <https://doi.org/10.1002/mma.8917>
32. *Boyer, F., Minjeaud, S.* Numerical schemes for a three component Cahn-Hilliard model // *ESAIM: Mathematical Modelling and Numerical Analysis*. 2011. V. 45. No. 4. pp. 697-738. <https://doi.org/10.1051/m2an/2010072>
33. *Brachet, M., Chehab, J.-P.* Fast and Stable Schemes for Phase Fields Models // *Computers & Mathematics with Applications*. 2020. V. 80. Iss. 6. pp. 1683-1713. <https://doi.org/10.1016/j.camwa.2020.07.015>
34. *Elliott, C., French, D.A.* A nonconforming finite element method for the two- dimensional Cahn–Hilliard equation // *SIAM J. Numer. Anal.* 1989. V. 26. No. 4. pp. 884–903. <https://www.jstor.org/stable/2157884>
35. *Barrett, J.B.* An error bound for the finite element approximation of the Cahn–Hilliard equation with logarithmic free energy // *Numer. Math.* 1995. Vol. 72. pp. 1–20. <https://doi.org/10.1007/s002110050157>
36. *Chen, L.-Q., Shen, J.,* Applications of semi-implicit Fourier-spectral method to phase field equations // *Comput. Phys. Commun.* 1996. V. 108. Iss. 2-3. pp. 147–158. [https://doi.org/10.1016/S0010-4655\(97\)00115-X](https://doi.org/10.1016/S0010-4655(97)00115-X)
37. *Furihata, D.* A stable and conservative finite difference scheme for the Cahn– Hilliard equation // *Numer. Math.* 2001. V. 87. Iss. 4. pp. 675–699. <https://doi.org/10.1007/PL00005429>
38. *Feng, X., Prohl, A.* Error analysis of a mixed finite element method for the Cahn– Hilliard equation // *Numer. Math.* 2004.V. 99. Iss. 1. pp. 47–84. <https://doi.org/10.1007/s00211-004-0546-5>
39. *Wells, E., Kuhl, K., Garikipati* A discontinuous Galerkin method for the Cahn– Hilliard equation // *J. Comput. Phys.* 2006. V. 218. Iss. 2. pp. 860–877. <https://doi.org/10.1016/j.jcp.2006.03.010>

40. *Wise, S.M., Wang, C., Lowengrub, J.S.* An Energy-Stable and Convergent Finite-Difference Scheme for the Phase Field Crystal Equation // *SIAM Journal on Numerical Analysis*. 2009. V. 47. Iss. 3. pp. 2269-2288. <https://doi.org/10.1137/0807381>
41. *Du, Q., Ju, L., Tian, L.* Finite element approximation of the Cahn–Hilliard equation on surfaces // *Computer Methods in Applied Mechanics and Engineering*. 2011. V. 200. Iss. 29–32. pp. 458-2470. <https://doi.org/10.1016/j.cma.2011.04.018>.
42. *Xia, Y., Xu, Y., Shu, C.-W.* Local discontinuous Galerkin methods for the Cahn–Hilliard type equations // *Journal of Computational Physics*. 2007. V. 227. Iss. 1. pp. 472-491. <https://doi.org/10.1016/j.jcp.2007.08.001>
43. *Brenner, S.C., Diegel, A.E., Sung, L.-Y.* A robust solver for a second order mixed finite element method for the Cahn–Hilliard equation // *Journal of Computational and Applied Mathematics*. 2020. V. 364. pp. 112322. <https://doi.org/10.1016/j.cam.2019.06.038>
44. *Gómez, H., Calo, V.M., Bazilevs, Y., Hughes, T.J.R.* Isogeometric analysis of the Cahn–Hilliard phase-field model // *Computer Methods in Applied Mechanics and Engineering*. 2008. V. 197, Iss. 49–50. pp. 4333-4352. <https://doi.org/10.1016/j.cma.2008.05.003>
45. *Zhang, R., Qian, X.* Triangulation-based isogeometric analysis of the Cahn–Hilliard phase-field model // *Computer Methods in Applied Mechanics and Engineering*. 2019. V. 357. pp. 112569. <https://doi.org/10.1016/j.cma.2019.112569>
46. *Kästner, M., Metsch, P., de Borst, R.* Isogeometric analysis of the Cahn–Hilliard equation — a convergence study // *Journal of Computational Physics*. 2016. V. 305. pp. 360-371. <https://doi.org/10.1016/j.jcp.2015.10.047>
47. *Goudenège, L., Martin, D., Vial, G.* High Order Finite Element Calculations for the Cahn–Hilliard Equation // *J. Sci. Comput.* 2012. V. 52. pp. 294–321 <https://doi.org/10.1007/s10915-011-9546-7>
48. *Čžao-Din, Y.* On the stability of difference schemes for the solutions of parabolic differential equations. (Russian), *Dokl. Akad. Nauk SSSR* 117, 578–581 (1957) <https://zbmath.org/?q=an:0102.33501>
49. *Čžao-Din, Y.* Some difference schemes for the numerical solution of differential equations of parabolic type. (Russian) *Mat. Sb. (N.S.)*, 50(92), (1960), 391–422. <https://www.mathnet.ru/eng/sm4800>
50. *Gel'fand I.M., Lokutsievskii O.V.* On difference schemes for solving the heat equation (Russian), In book: *Godunov S.K., Ryaben'kii V.S., Introduction to the theory of difference schemes*, Gosudarstv. Izdat. Fiz.-Mat. Lit., Moscow, 1962, 340 pp.
51. *Babenko, K. I.* Foundations of numerical analysis (Russian), Publisher “Regular and chaotic dynamics”, Izhevsk, 2002, 848 pp.
52. *Lokutsievskii V.O., Lokutsievskii O.V.* Application of Chebyshev parameters to numerical solution of some evolution problems (Russian), *KIAM Preprint № 99*, Moscow, 1984, 30 pp. <https://library.keldysh.ru/preprint.asp?id=1984-99>

53. *Zhukov V.T.* Numerical experiments for solving the heat equation by the local iteration method (Russian), KIAM Preprint № 97, Moscow, 1984, 22 pp. <https://library.keldysh.ru/preprint.asp?id=1984-97>
54. *Lokutsievskii, V.O., Lokutsievskii, O.V.* On numerical solution of boundary value problems for equations of parabolic type. *Sov. Math. Dokl.* 34(3), 512–516 (1987) <https://www.mathnet.ru/eng/dan47741>
55. *Zhukov V.T.* Local iteration difference schemes for parabolic equations (Russian), KIAM Preprint № 173, Moscow, 1986, 31 pp. <https://library.keldysh.ru/preprint.asp?id=1986-173>
56. *V.T. Zhukov* Explicit Iteration Schemes for Parabolic Equations (Russian), *Vopr. Atomm. Nauki I Tekn., Ser. Mat. Mod. Fiz. Proc.*, No. 3, pp. 40–46 (1993).
57. *Shvedov, A.S., Zhukov, V.T.* Explicit iterative difference schemes for parabolic equations // *Russian J. Numer. Anal. Math. Modelling.* 1998. V. 13. № 2. pp. 133–148.
58. *Zhukov, V.T.* Explicit methods of numerical integration for parabolic equations. *Math. Models Comput. Simul.*, 3, pp. 311–332 (2011). <https://doi.org/10.1134/S2070048211030136>
59. *Zhukov V.T., Novikova N.D., Feodoritova O.B.* On application of multigrid and explicit-iterative methods to solution of the parabolic equations with anisotropic discontinuous coefficients (Russian). KIAM Preprint № 85, Moscow, 2014, 24 pp. <https://library.keldysh.ru/preprint.asp?lg=e&id=2014-85>
60. *Zhukov V. T., Feodoritova O. B., Duben A.P., Novikova N.D.* Explicit time integration of the Navier-Stokes equations using the local iteration method (Russian). KIAM Preprint № 12, Moscow, 2019, 32 pp. <https://library.keldysh.ru/preprint.asp?lg=e&id=2019-12>
61. *Zhukov, V.T., Feodoritova, O.B.* On Development of Parallel Algorithms for Solving Parabolic and Elliptic Equations. *J. Math. Sci.* 254, 606–624 (2021). <https://doi.org/10.1007/s10958-021-05329-y>
62. *Zhukov, V.T., Zaitsev, N.A., Lysov, V.G. et al.* Numerical analysis of a model of metal solidification, 2D case. *Math Models Comput Simul* 4, 440–453 (2012). <https://doi.org/10.1134/S2070048212040096>
63. *Lee, D., Huh, J.-Y., Jeong, D., Shin, J., Yun, A., Kim, J.* Physical, mathematical, and numerical derivations of the Cahn–Hilliard equation // *Computational Materials Science.* 2014. V. 81. pp. 216–225. <https://doi.org/10.1016/j.commatsci.2013.08.027>
64. *Lee, S., Lee, C., Lee, H., Kim, J.* Comparison of different numerical schemes for the Cahn–Hilliard equation // *Journal of the Korea Society for Industrial and Applied Mathematics.* 2013. V. 17. Iss. 3. pp. 197–207. <https://doi.org/10.12941/jksiam.2013.17.197>
65. *Botchev M.A., Zhukov V.T.* Adaptive iterative explicit time integration for nonlinear heat conduction problems. *Lobachevskii J Math* 45, 12–20 (2024). <https://doi.org/10.1134/S1995080224010086>